doi:10.1093/plphys/kiab186 PLANT PHYSIOLOGY 2021: 186: 2190–2204

Plant Physiology®

Research Article

MITOGEN-ACTIVATED PROTEIN KINASE 4 impacts leaf development, temperature, and stomatal movement in hybrid aspen

Damian Witoń,[1] Marzena Sujkowska-Rybkowska ,[2] Joanna Dąbrowska-Bronk,[3] Weronika Czarnocka ,[2] Maciej Bernacki ,[4] Magdalena Szechyńska-Hebda[5,6] and Stanisław Karpiński[1,*,†]

1 Department of Plant Genetics, Breeding and Biotechnology, Institute of Biology, Warsaw University of Life Sciences, Warsaw 02776, Poland
2 Department of Botany, Institute of Biology, Warsaw University of Life Sciences, Warsaw 02776, Poland
3 Department of Plant Physiology, Institute of Biology, Warsaw University of Life Sciences, Warsaw 02776, Poland
4 Institute of Technology and Life Sciences, Raszyn 05090, Poland
5 The Franciszek Górski Institute of Plant Physiology, Polish Academy of Sciences, Cracow 30239, Poland
6 The Plant Breeding and Acclimatization Institute, National Research Institute, Błonie 05870, Poland

*Author for communication: stanislaw_karpinski@sggw.edu.pl
†Senior author.

S.K. and M.S.H. conceived the research plans and supervised the experiments; D.W. conceived the original screening and performed the experiments focusing on stomatal bioassays, modulated chlorophyll fluorescence measurements, RT-PCR analysis, foliar temperature measurements, nitric oxide signaling, and stress treatments, M.S.R. performed the experiments using the TEM microscopy; J.D.B. and W.C. performed RT-PCR and bioinformatics analysis; M.B. performed foliar temperature measurements and high light treatments; M.S.H. performed the experiments on hydrogen peroxide accumulation and microscopic analysis of stem cross section; D.W., M.S.H., and S.K. designed the experiments, analyzed the data and wrote the article; M.S.H. and S.K. conceived the project, supervised, and completed the writing. S.K. agrees to serve as the author responsible for contact and ensures communication.

The author responsible for distribution of materials integral to the findings presented in this article in accordance with the policy described in the Instructions for Authors (https://academic.oup.com/plphys/pages/general-instructions) is: Stanisław Karpiński (stanislaw_karpinski@sggw.edu.pl).

Abstract

Stomatal movement and density influence plant water use efficiency and thus biomass production. Studies in model plants within controlled environments suggest MITOGEN-ACTIVATED PROTEIN KINASE 4 (MPK4) may be crucial for stomatal regulation. We present functional analysis of MPK4 for hybrid aspen (*Populus tremula* × *tremuloides*) grown under natural field conditions for several seasons. We provide evidence of the role of MPK4 in the genetic and environmental regulation of stomatal formation, differentiation, signaling, and function; control of the photosynthetic and thermal status of leaves; and growth and acclimation responses. The long-term acclimation manifested as variations in stomatal density and distribution. Short-term acclimation responses were derived from changes in the stomatal aperture. MPK4 localized in the cytoplasm of guard cells (GCs) was a positive regulator of abscisic acid (ABA)-dependent stomatal closure and nitric oxide metabolism in the ABA-dependent pathways, while to a lesser extent, it was involved in ABA-induced hydrogen peroxide accumulation. MPK4 also affected the stomatal aperture through deregulation of microtubule patterns and cell wall structure and composition, including via pectin methyl-esterification, and extensin levels in the GC wall. Deregulation of leaf anatomy (cell compaction) and stomatal movement, together with increased light energy absorption, resulted in altered leaf temperature, photosynthesis, cell death, and biomass accumulation in *mpk4* transgenic plants. Divergence between absorbed energy and assimilated energy is a bottleneck, and MPK4 can

Received January 19, 2021. Accepted April 2, 2021. Advance access publication May 19, 2021

participate in the control of energy dissipation (thermal effects). Furthermore, MPK4 can participate in balancing the photosynthetic energy distribution via its effective use in growth or redirection to acclimation/defense responses.

Introduction

Plants are sessile organisms that lack opportunities to avoid environmental stress. Their survival and productivity depend on efficient perception of and response to constantly changing environmental factors and intracellular signals.

Stomatal guard cells (GCs) play a role in sensing and responding to environmental factors (e.g. changes in CO_2, temperature, light, and humidity) by internal control of stomatal development and externally induced rapid adjustment of the stomatal aperture. They participate in the regulation of photosynthesis, CO_2 assimilation, energy dissipation, and transpiration. The mechanisms that regulate stomatal functioning have been studied intensively (Shimazaki et al., 2007; Kim et al., 2010). The processes leading to the proper development and distribution of the stomata include asymmetric division, cell fate specification, and establishment and maintenance of stem cell populations. Opening and closing are achieved by the swelling and shrinking of GCs, which is driven by ion exchange, cytoskeleton reorganization, and metabolite production. Stomatal cell walls undergo reversible deformation during opening/closing of the pore, and thus, a suitable composition of the cell wall and its strength and flexibility are important for efficient functioning of stomata. All of these processes are dependent on the modulation of gene expression and the posttranslational modification of various proteins (reviewed in Kim et al., 2010), but they are also strongly influenced by environmental factors (Zoulias et al., 2018).

GCs integrate endogenous and environmental stimuli into signaling networks that regulate plant growth, photosynthesis, photorespiration, cell death, and abiotic and biotic stress responses. Among other factors, mitogen-activated protein kinases (MAPK or MPK), evolutionarily conserved regulatory molecules (Pitzschke et al., 2009; Rodriguez et al., 2010), play a role in GC development, immune responses, abscisic and salicylic acid (ABA and SA) signaling, and biotic or abiotic stress response (Gawroński et al., 2014, 2021). MPK4 was initially identified in Arabidopsis (*Arabidopsis thaliana*) as a negative regulator of systemic acquired resistance (SAR) together with SA and reactive oxygen species (ROS) as key players. MPK4 has also been described as a regulator involved in cytokinesis, reproduction, and photosynthesis (Zeng et al., 2011; Hettenhausen et al., 2012). Although MPK4 is highly abundant in GCs, its role in stomatal movement seems controversial. In *Nicotiana attenuata*, MPK4 is required for ABA-mediated stomatal closure after drought stress (Hettenhausen et al., 2012). In contrast, *MPK4*-silenced *Nicotiana tabacum* plants had normal ABA-induced stomatal movements (Gomi et al., 2005; Marten et al., 2008), but CO_2- and dark-induced stomatal closure was disturbed (Marten et al., 2008). *MPK4*-silenced plants of *Populus tremula* × *tremuloides* exhibited elevated stomatal conductance and transpiration intensity compared with wild-type (WT) plants, and the presence of MPK4 was crucial for control of photosynthesis, cell wall thickening, and plant growth by modulating ROS/hormonal homeostasis (Witoń et al., 2016). Recently, Töldsepp et al. (2018) showed that MPK4 and MPK12 are essential coregulators of high-CO_2-triggered stomatal closure and low-CO_2-mediated stomatal opening. Moreover, MPK4 was identified as a protein that can directly sense CO_2 (Gałgańska and Gałgański, 2020). Altogether, these results suggest that MPK4 may be crucial for the regulation of stomatal movements and/or density, influencing water use efficiency and thus biomass production.

However, all functional MPK4 analyses were performed so far in annual model plants cultivated in laboratory condition. Although much has been learned from laboratory experiments, a comprehensive understanding of gene function also requires studies in the natural environment (Wituszyńska et al., 2013). Bearing in mind that modern plant genomes have been evolving for millions of years and carry a genetic record of their adaptations, measuring the effect in the natural environment especially in perennial plants like trees ensures a real estimate of the gene function and its consequence on plant fitness and productivity. Our experiments demonstrate multilevel MPK4 function in stomatal and leaf development, in regulation of photosynthesis and cellular signaling, thus in the photosynthetic and thermal status of the leaves, and in growth and acclimation responses.

Results

Deregulated leaf and stomatal structure in *mpk4* plants

To test the function of MPK4, an anatomical and ultrastructural characterization of hybrid aspen leaves was performed for WT (T89) plants and two transgenic lines grown in the field conditions (Supplemental Figure S1): *mpk4*-5 (reduced expression of *MPK4* to ∼75%) and *mpk4*-7 (reduced expression of *MPK4* to ∼10%). WT, *mpk4*-5, and *mpk4*-7 leaves exhibited typical epidermal layers in adaxial (upper) and abaxial (lower) leaf surfaces, two layers of palisade parenchyma (PP), spongy parenchyma tissue, and vascular bundle systems (Figure 1, A–C). Different cell sizes were observed in leaf cross-sections; WT plants had larger cells of all tissue types, while smaller cells were found for both *mpk4* genotypes (Figure 1, A–C; Supplemental Table S1). Particularly small cell diameters were observed in the PP and abaxial leaf epidermis, including for stomatal GCs (Figure 1, A–F).

The specific function of MPK4 in GCs was confirmed in hybrid aspen WT leaves with an anti-MPK4 primary antibody and anti-rabbit secondary IgG antibody conjugated with FITC-isomer (Supplemental Figure S2). Indirect immunofluorescence with confocal laser scanning microscopy imaging demonstrated that the MPK4 protein in GCs was localized exclusively in the cytoplasm, not in the cell wall or vacuoles. Therefore, the strong differences in stomatal development and functioning were not surprising. Different plants can develop stomata on only the abaxial surface of the leaf (hypostomatous) or on both abaxial and adaxial surfaces (amphistomatous), and heritable variation was detected among *Populus* species and clones (Dillen et al., 2008). In the case of aspen, the amphistomatous leaf type was found in Figure 1, A–I); however, all plants had a higher number of stomata in the abaxial epidermis than in the adaxial epidermis (Figure 1J). Compared to the WT, *mpk4* transgenic lines had a higher number of stomata in both the abaxial and abaxial epidermises, but the improvement in the adaxial epidermis was statistically more significant. Although the cell number in *mpk4* leaves increased ~120%–160% in comparison to that in WT leaves (Supplemental Table S1); thus, the intercellular space was reduced greatly (Figure 1, A–C; mostly, but not exclusively, the intercellular space adjacent to the adaxial epidermis), and the number of stomata was improved to a greater extent, by 300% and 500% for *mpk4*-5 and *mpk4*-7, respectively (Figure 1J).

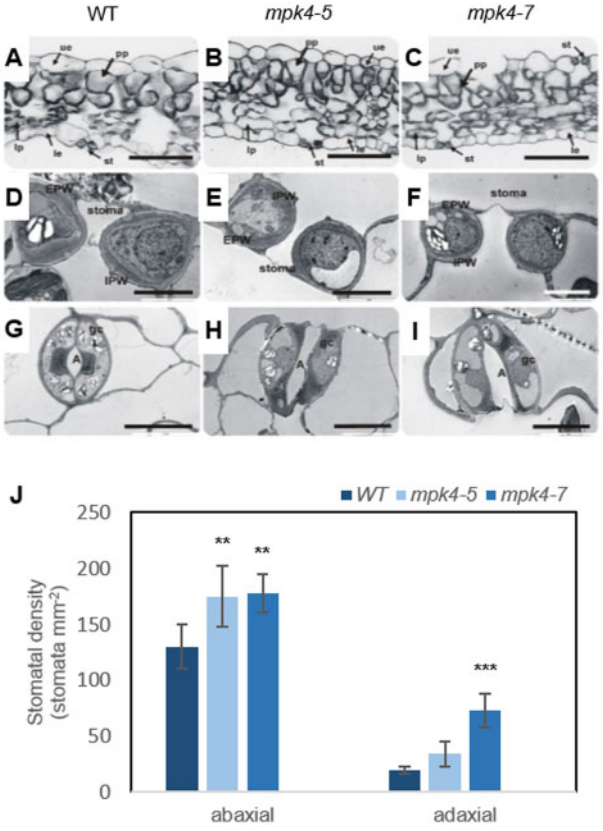

Figure 1 Leaf development, stomatal ultrastructure, and stomatal density were dependent on MPK4. Microscopic analysis was performed for WT and transgenic *mpk4*-5 and *mpk4*-7 plants. A–C, Light micrographs of a leaf cross-section. le, lower epidermis; lp, lacunous parenchyma; st, stoma; ue, upper epidermis. D–F, Transmission electron micrographs showing a median transverse section of a stoma. G–I, Paradermal sections of guard cells from the le. A, aperture; EPW, external periclinal wall; IPW, internal periclinal wall. Scale bars: (A–C) 50 μm; (D–F) 5 μm; (G–I) 10 μm. J, Mean stomatal density ± SD ($n = 3$) of the epidermal layer in adaxial (upper) and abaxial (lower) leaf surfaces. The asterisks indicate significant differences from the WT revealed by Tukey's HSD test; $^{**}P < 0.01$, $^{***}P < 0.001$.

With regard to the GC ultrastructure, WT stomatal walls showed irregular thickening. The thickest cell wall near the pore and the thinnest cell wall between the GC and the neighboring cell were observed for the WT (Figure 1, D and G). In *mpk4*-5 and *mpk4*-7, the cell walls were thinner compared to that in WT, and their thickness was regular around the whole perimeter (Figure 1, E, F, H, and I). The results suggested that cell wall composition can be significantly influenced by MPK4. Indeed, immunolocalization analyses of *mpk4-7* GCs revealed a major change in the homogalacturonan (HG) domain of pectic polysaccharides and methyl-esterification status of the pectin wall (JIM5 and JIM7 antibodies), unesterified pectin abundance (JIM5), and localization of extensins (JIM12; Figure 2; Supplemental Figure S3). Weaker binding of each antibody was found in *mpk4* cells than in WT cells. Similarly, MPK4 was implicated in the distribution of microtubules (MTs; Supplemental Figure S4), which are a prerequisite for proper cell division and growth, as a network for stabilization and macromolecule supply (Szechyńska-Hebda et al., 2006); proper cell wall biosynthesis, by governing cellulose microfibril orientation; and proper GC movement, by polymerization/depolymerization of transversally oriented cortical MTs during GC opening/closure (Swamy et al., 2015). A clear MT pattern was found in the WT GCs, mainly in the peripheral part of the cytoplasm, while specific MT organization in *mpk4-7* GCs was not detected because fluorescence was scattered throughout the cytoplasm (Supplemental Figure S4). Regular cell wall thickness (Figure 1, D–F), modified cell wall composition (Figure 2; Supplemental Figure S2), and MT functioning (Supplemental Figure S4), together with higher cell vacuolization (Figure 1, D–F), resulted in a rounder shape of *mpk4* GCs in comparison to WT cells in cross-sections (Figure 1, D–F; Supplemental Table S1) and in more open *mpk4* stomatal pores when the epidermal surface was analyzed (Figure 2; Supplemental Figure S3).

Although *MPK4* downregulation in transgenic plants affected all leaf tissues, we conclude that the highest impact of genetic modification was found for the cellular and subcellular structures of GCs, suggesting dysfunction of stomatal closure and its alteration and, consequently, in deregulation of leaf physiology and finally in plant biomass accumulation.

Dysfunction of stomatal closure and alteration in *mpk4* plants

MPK4 downregulation in transgenic plants decreased the transcript level of the constitutively photomorphogenic

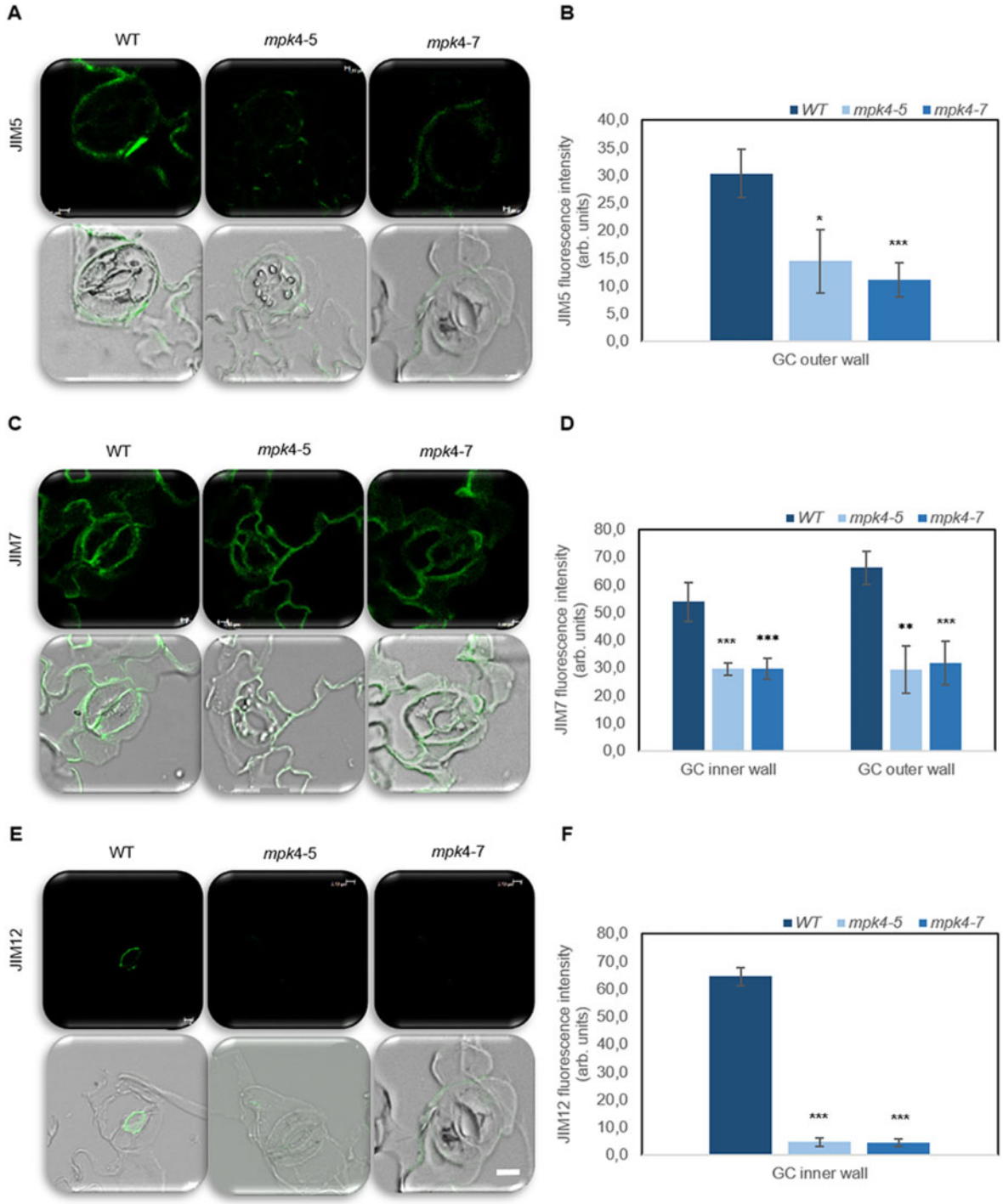

Figure 2 Pectin composition and extensin level in WT and transgenic mpk4-5 and mpk4-7 GC walls. The green signal is the signal from the antibody conjugated to FITC. An overlay between the green antibody signal and bright-field is also presented. The JIM5 antibody (A–B) recognizes the HG domain of pectic polysaccharides, partially methyl-esterified epitopes of HG, and unesterified HG. The JIM7 antibody (C–D) recognizes the HG domain of pectic polysaccharides, partially methyl-esterified epitopes of HG but not unesterified HG. The extensins are indicated by the JIM12 antibody (E–F). Scale is uniform for each photo, scale bar: 2 μm. Control without primary antibody was made for each type of sample to confirm the lack of signal (Supplemental Figure S3). The presented pictures are representative of 10 analyses ±SDS ($n = 30$). Fluorescence was measured using Leica confocal software and is expressed as arbitrary units. The asterisks indicate significant differences from the WT revealed by Tukey's HSD test; *$P < 0.05$, **$P < 0.01$, ***$P < 0.001$.

1 (*COP1*) gene, a key repressor of photomorphogenesis (Figure 3A). In contrast, *MPK4* downregulation increased the expression of marker genes known to encode proteins responsible for environmental control of stomata; development, such as cryptochrome 1 and 2 (CRY1 and CRY2), phytochrome A (phyA), or transcription factors crucial for

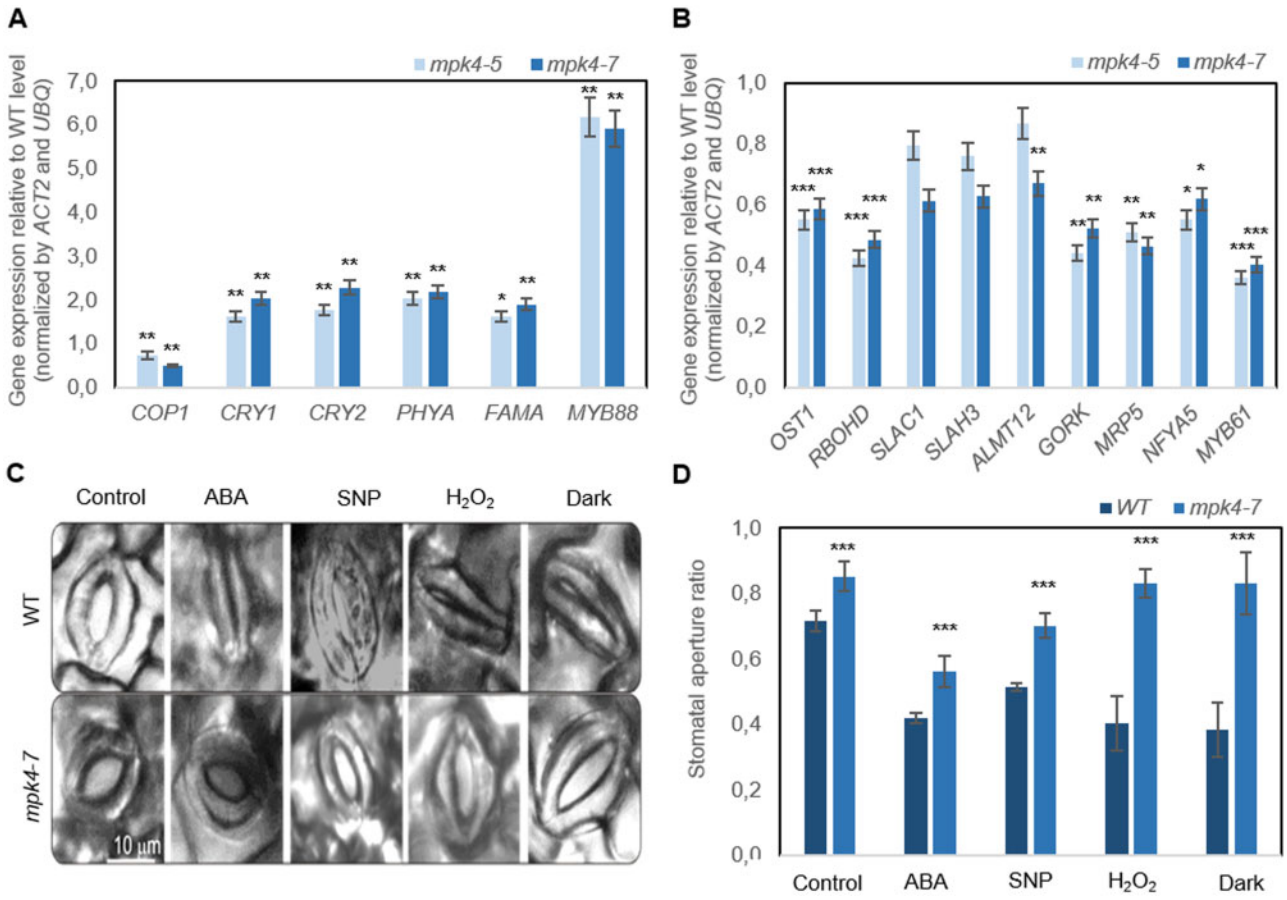

Figure 3 Regulation of stomatal development and function in WT and transgenic *mpk4-5 and mpk4-7* plants. A, Expression pattern of genes encoding proteins responsible for environmental control of stomatal development. B, Expression of genes encoding core components of the ABA signaling pathways in stomata. The expression level for (A) and (B) is presented relative to the level in the WT, referred to as 1.0. Presented values are means ± SDS ($n = 6$). C, Stomatal aperture in the WT and *mpk4-7* plants after ABA, SNP (NO donor), H_2O_2, and dark treatments presented as representative microphotographs. D, Corresponding stomatal aperture ratio (stomata width/stomata length). C–D, Samples treated with "opening solution" in light conditions were used as a control (for details see "Materials and methods"). The values are the means ± SDS ($n = 6$) of three independent experiments. The asterisks indicate significant differences from the WT revealed by Tukey's HSD test; $^*P < 0.05$, $^{**}P < 0.01$, $^{***}P < 0.001$.

environmentally dependent cell division and stomata formation, such as FAMA and MYB88. This result indicated an influence of MPK4 on stomatal responsiveness to abiotic stress conditions. This was confirmed by analysis of the contribution of cis-regulatory elements (CREs; specific noncoding DNA motifs) to promoter activity, which was determined by different environmental stimuli, that is, high and low temperature, CO_2, light (high light, red light [RL], red/blue light [RL/BL], drought, and endogenous phytohormonal (auxin, gibberellin, and SA) regulation (Supplemental Figure 5A; Supplemental Tables S2 and S3). Furthermore, the results obtained during in silico promoter analysis were experimentally validated, and it was shown that the *MPK4* expression level in WT hybrid aspen plants was increased by low temperature (4°C), high CO_2 (HCO_2) levels (2,000 ppm), and darkness but reduced by high temperature (42°C), high light intensity (photons of 2,000 µmol m^{-2} s^{-1}), RL, and RL supplemented with BL (Supplemental Figure S5B).

To confirm that the involvement of MPK4 in stomatal closure was dependent on ABA, the expression of related genes was analyzed in *mpk4* plants (Figure 3B). The reduction in *MPK4* expression in transgenic lines led to downregulation of genes encoding ABA-responsive protein kinase (open stomata 1 [OST1]) and NADPH oxidase catalytic subunit D (ATRBOHD), both of which are responsible for ABA-triggered ROS generation in GCs (Kwak et al., 2003); S-type anion channel 1 (SLAC1), S-type anion channel homolog 3 (SLAH3), aluminum-activated malate transporter 12 (ALMT12), and outward K+ channel (GORK), which are GC membrane transporters; an ATP-binding cassette transporter (MRP5) mediating solute transport; and nuclear factor Y proteins (such as NFYA5) and MYB domain proteins (such as MYB61), which are important regulators of stomatal movement (Gray, 2005; Cominelli et al., 2010). These genes (Figure 3B) are preferentially expressed in Arabidopsis GCs, but up to today the selected markers were not confirmed as GC-expressed genes in aspen. Although the total RNA was

isolated from the whole leaf, the role of genes was clearly related to the MPK4-dependent of stomata closure. Additionally, the stomata stayed open permanently in response to ABA treatment and dark conditions (Figure 3, C–D). Similarly, hydrogen peroxide (H_2O_2) and nitric oxide (NO), identified as key molecules regulating ABA- and dark-induced stomatal closure (Bright et al., 2006; Neill et al., 2008), did not enable stomatal closure (Figure 3, C–D). In contrast, WT stomata were closed in most conditions. The exception was treatment with sodium nitroprusside (SNP; an NO donor); WT stomata were not closed completely. However, stomatal closure after SNP application was still more pronounced in the WT than in the transgenic leaves. Exogenous application of ABA-induced H_2O_2 production in the GC cytoplasm of WT and *mpk4-7* cells at a similar level (Supplemental Figure S6A); thus, MPK4 might indirectly affect H_2O_2 generation in GCs. ABA and SNP treatments also induced NO production in the cytoplasm of GCs; however, in both cases, NO accumulation in *mpk4-7* GCs was lower than that in WT GCs (Supplemental Figure S6, B–C). NO production peaked within a few minutes (Supplemental Figure S6C, while stomatal closure was completed after 2 h (Figure 3C); thus, we suggested that MPK4 functioned upstream of NO production in the ABA-dependent stomatal response.

Deregulated leaf functioning and plant biomass accumulation

The temperature of the leaf surface, measured continuously and nondestructively with infrared thermography, showed that both transgenic *mpk4* plants had temperatures higher by $\sim 2^{\circ}C$ than that of the WT in dark conditions (Figure 4, A–B). In response to light, the differences increased, reaching 3.5°C, 4.0°C, and 6.0°C, at light intensities of 375, 750, and 1,500 µmol m^{-2} s^{-1}, respectively. Transgenic plants were expected to have a lower leaf temperature as the result of permanently opened stomata; however, apparently, the increased temperature could be the reason why stomata preferentially remain open. Upon searching for an explanation, we found that the stress imposed by H_2O_2 accumulation in leaf tissue was evident for *mpk4* plants (Figure 4C; Supplemental Figure S7). Staining with 3,3′-diaminobenzidine (DAB) could be observed more clearly in both mesophyll and vein tissues of *mpk4* leaves. Along with H_2O_2 overproduction, higher dissipation of light energy (Figure 5A; DI_0/RC, φD_0), which was more strongly absorbed from light flashes (Figure 5A; ABS/RC), suggested greater requirement for the induction of protective responses in leaf cells. H_2O_2 accumulation could result, at least in part, from the higher photosynthetic electron transport and trapped energy flux (Figure 5A; ET_0/RC, TR_0/RC), justifying a role of the dissipation mechanism in protecting *mpk4* plants against photosystem II (PSII) photoinhibition. Another mechanism induced under stress and related to H_2O_2 and cell death regulation consists of the repair and reassembly of PSII proteins during their damage or the early steps of de novo assembly of PSII (Dyda et al., 2019). The light-harvesting chlorophyll a/b binding proteins (Lhcb), the functional redistribution of which is required to harvest light energy efficiently and balance the relative excitation of PSII and PSI, were divergently regulated at the gene expression level (Figure 6A). However, the *Lhcb1* gene product, which is the most abundant (Pietrzykowska et al., 2014), was upregulated in *mpk4* plants compared with WT plants. The upregulation of this gene was higher in the *mpk4-7* plants, which showed the lowest *MPK4* expression. Similarly, the expression of genes encoding an oxygen-evolving enhancer protein 1-1 (PsbO1), which was proposed to play a central role in the stabilization of the catalytic manganese cluster, as well as an oxygen-evolving enhancer protein 3-1 (PSBQA), required for PSII assembly/stability, was induced in *mpk4* plants. Furthermore, some of the genes encoding a heat shock transcription factor (HSF; HSFA1a) and heat shock proteins (HSPs; HSP70, HSP90), known to directly sense abiotic stress and H_2O_2 via the engagement of the redox state (Swindell et al., 2007; Liu et al., 2013), were induced in *mpk4* leaves (Figure 6B). In particular, a change of more than two-fold in the expression of HSPs was noteworthy. All of the above-described mechanisms could be important during exposure of plants to destructive stress, as indicated by reduced ion leakage in *mpk4* plants in comparison to WT plants under high-temperature stress (Figure 6C; 25°C versus 42°C), and are thus required for protecting plants from cell death. The decreased expression of the *MPK4* gene in WT plants at high temperatures (Figure 6D) supports the statement that MPK4 expression should be reduced to induce acclimation responses. On the other hand, the quantum yield of the primary PSII photochemistry and electron transport (Figure 5A; φP_0, $\varphi E0$, F_v/F_0, ψ_0), CO_2 assimilation process (Figure 5A; P.I.), and accumulation of biomass in the form of wood formation in the stem (Figure 5B; Supplemental Figure S8) were impaired in *mpk4* leaves.

Discussion

Two transgenic aspen lines, namely, *mpk4*-5 and *mpk4*-7, with reduced *MPK4* expression cultivated in four vegetative seasons in field conditions displayed increased transpiration, decreased water use efficiency, and impaired plant growth (Witoń et al., 2016). Therefore, in the present work, the following hypotheses were verified: (1) MPK4 functions in GCs and influences stomatal development and/or movement; (2) MPK4-dependent long-term acclimation to fluctuating field conditions is manifested through changes in stomatal density; (3) MPK4-dependent short-term response to fluctuating field conditions derives from changes in the stomatal aperture and conductance; (4) deregulation of stomatal development and function is a key factor determining transgenic plant physiology (photosynthesis, energy conversion, and distribution) and eventually plant growth in fluctuating field conditions; and (5) MPK4 is an important multifaceted kinase that functions in many processes involved in developmental and acclimation responses. The role of MPK4 in GCs

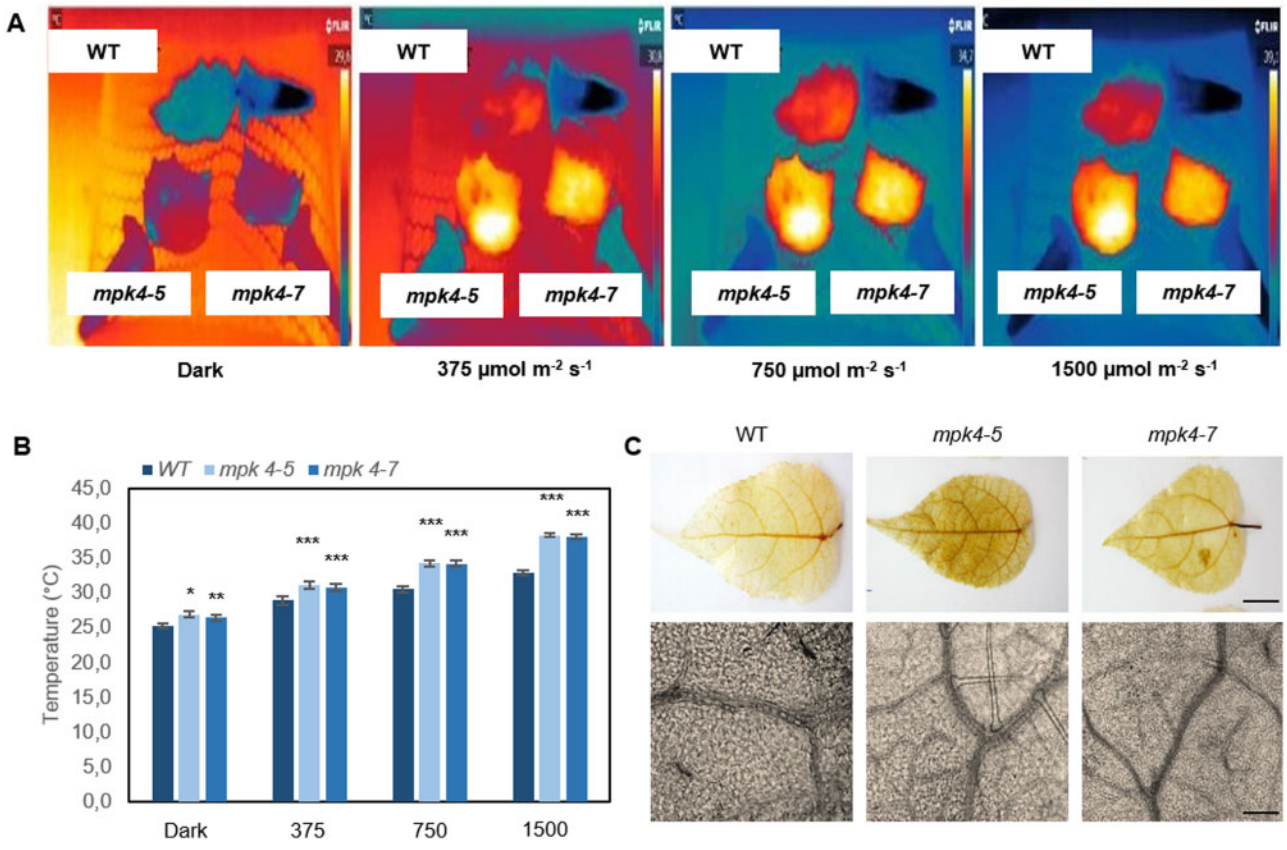

Figure 4 Leaf temperature and H_2O_2 accumulation in WT and transgenic *mpk4-5* and *mpk4-7* plants. A, Pictures made with a thermographic camera (T650sc, FLIR). Plants grown in field conditions were dark-adapted and exposed to light intensities of 375, 750, and 1,500 µmol m^{-2} s^{-1} (LED Lamp SL 3500-W, PSI); the 3-min illumination periods were separated by a period of darkness lasting 1 min. During thermographic measurements, leaf petioles were immobilized in Eppendorf tubes filled with water. B, Leaf temperature recorded for each light period. The values are the means ± SDS ($n = 6$) of three independent experiments. The asterisks indicate significant differences from the WT revealed by Tukey's HSD test; $^*P < 0.05$, $^{**}P < 0.01$, $^{***}P < 0.001$. C, H_2O_2 accumulation visualized with histochemical DAB staining in a whole leaf (magnitude 20×) and leaf fragments (100×). Scale bars: 1 cm and 0.25 mm.

was previously studied in *N. tabacum* (Gomi et al., 2005; Marten et al., 2008), *N. attenuata* (Hettenhausen et al., 2012), and Arabidopsis (Colcombet et al., 2013) cultivated in the laboratory conditions; however, no reports have been published regarding the role of MPK4 in woody perennial plants growing for several seasons in variable field conditions. Similarly, molecular regulators and plant responses are usually studied under stable laboratory conditions, whereas they are fully expressed only in environments associated with multiple stresses (Wituszyńska et al., 2013). We present the first functional analysis of MPK4 under natural conditions.

The traits for hybrid aspen lines grown in natural field conditions during four seasons showed gradations along with downregulation of the *MPK4* gene in most cases. This indicates that the changes in the traits were the result of their deregulation, not of the site of the transformation event. The results indicated that MPK4 was localized in the WT cytoplasm of GCs but not in the GC wall, GC vacuoles, or other leaf tissues (mesophyll, veins). Despite the restricted location, MPK4 influences whole stomatal ultrastructure, as transgenic lines with reduced *MPK4* expression had significantly modified GC walls, vacuoles, and MTs, as well as whole-leaf anatomy, including cell size, number, and compaction. However, the stomatal number was improved to a greater extent (300%–500% of WT) than the cell number (120%–160% of WT) in *mpk4* leaves. One can consider whether such a high stomatal density is associated with a dense internal tissue of the leaf (small cells, a more compact arrangement of mesophyll cells, a network of very small intercellular spaces in the *mpk4* plants). In dense tissues, gas exchange and photosynthetic efficiency (mainly CO_2 assimilation) are reduced; thus, the increased number of stomata should alleviate negative effects and increase CO_2 and H_2O distribution in the leaves. There is no consensus regarding whether changes in CO_2 constitute direct stress, but emerging evidence suggests that while CO_2 is a substrate, it can also be a signal mediating the plant response (Foyer and Noctor, 2020), and the evolutionary trend across plant species is to increase stomatal density with decreasing levels of atmospheric CO_2. Conversely, when plants are grown in high levels of CO_2, the stomatal density decreases (Brownlee,

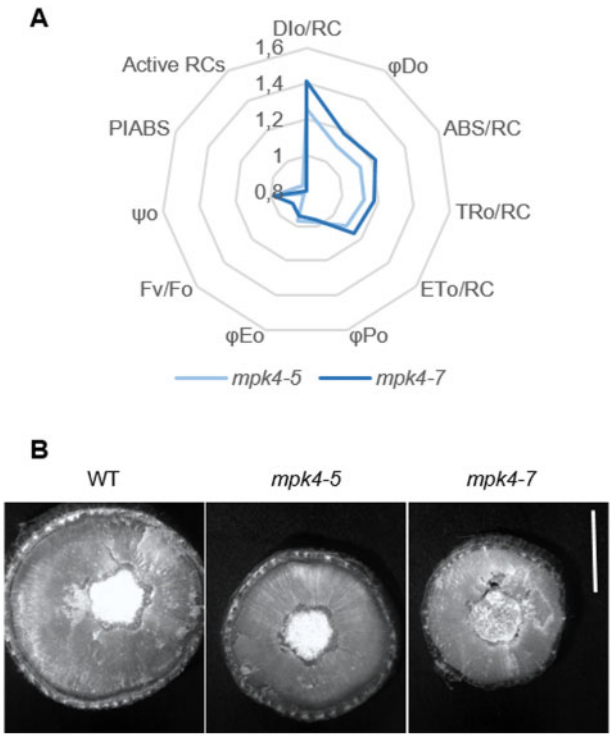

Figure 5 Photosynthetic performance and biomass accumulation in WT and transgenic *mpk4-5* and *mpk4-7* plants. A, Mean changes in chlorophyll *a* fluorescence parameters measured by the OJIP test: DI_0/RC, dissipated energy flux per RC; φD_0, quantum yield (at $t = 0$) for energy dissipation; ABS/RC, absorption flux per *RC*; TR_0/RC, trapped energy flux per RC; ET_0/RC, electron transport flux per RC; φP_0, maximum quantum yield of the primary PSII photochemistry; φE_0, quantum yield of electron transport (at $t = 0$); F_v/F_0, PSII potential activity; ψ_0, probability (at $t = 0$) that a trapped excitation moves an electron into the electron transport chain beyond QA; PI_{ABS}, the performance index; Active RCs, relative number of active RCs. Parameters are presented relative to the WT, referred to as 1.0 ($n = 6$). The parameters DI_0/RC, φD_0, ABS/RC, TR_0/RC, and ET_0/RC for both *mpk4* lines are significantly different from those for the WT, as revealed by the Tukey's HSD test; $^{***}P < 0.001$. B, Cross-section of a stem at ~100 cm from the apex of the plant photographed under a microscope. Scale bar: 5 cm.

2001). Thus, the decrease in internal CO_2 concentration in dense leaf tissue can also be the factor influencing improved stomatal development and distribution. Although it seems that MPK4 is involved in stoma-dependent regulation of plant metabolic responses in a fluctuating environment, improvement in the number of stomata was not enough as a long-term acclimation response that can prevent a reduction in the quantum yield of the primary PSII photochemistry and electron transport (φP_0, $\varphi E0$, F_v/F_0, ψ_0), an increase in leaf temperature, and a decrease in plant biomass, particularly wood tissue in the stem.

MPK4 influenced changes in stomatal development, which, in turn, led to short-term stomatal responses under sudden stress, for example, deregulation of stomatal movement. Drastic cell wall modification was found in *mpk4* transgenic plants: a thinner and regular cell wall around the whole perimeter of GCs; modified cell wall chemical composition, at least in the HG domain of pectic polysaccharides; and increased abundance of methyl-esterified pectins, unesterified pectin, and extensins. Pectin is synthesized in methyl-esterified form and is de-esterified in muro by pectin methyl esterases (Lionetti et al., 2012; Amsbury et al., 2016). Both unesterified pectin and highly methyl-esterified pectin were present in the cell walls of WT and *mpk4* GCs. However, an alteration in the methyl-esterification status was found in the cell wall of *mpk4* GCs. In contrast, a change in the overall distribution of HG did not simply reflect the changes in the patterns of cell wall thickness or overall distribution of cellulose in the WT. More significant changes that are of great importance for the functioning of *mpk4* stomata occurred in the network of extensins. Extensins form positively charged scaffolds that are important for cell wall self-assembly (Cannon et al., 2008). The reduction in extensins in *mpk4* GCs, in the part of the cell wall directly surrounding the stomatal pore, led to incomplete cross wall assembly and reduced cell wall thickness, and to inhibited stomatal movement as the outcome. It can be concluded that cell wall modification also occurred at earlier steps, before the formation process in transgenic *mpk4*. Cortical MT arrays direct the deposition patterns of cell walls at the plasma membrane during cell division and cytokinesis (Szechyńska-Hebda et al., 2006); thus, deregulated orientation and/or polymerization of MTs irrevocably led to improper cell wall differentiation in *mpk4* GCs and thus deregulated stomatal movement. MPK4 downregulation also increased GC vacuolization, which also supported the round shape of GCs. In addition to structural properties, many other mechanisms of stomatal movement were altered in transgenic *mpk4* plants: (1) the transcript levels of a photomorphogenesis repressor (*COP1*) decreased, while the expression of genes responsible for environmental control of stomatal division, formation, and development (*CRY1*, *CRY2*, *PHYA*, *FAMA*, *MYB88*) increased; (2) the expression of genes related to ABA-dependent signaling (*OST1*), genes related to ABA-triggered ROS generation in GCs (*ATRBOHD*; Kwak et al., 2003), genes related to GC membrane transport, stomatal turgor and volume (*SLAC1*, *SLAH3*, *ALMT12*, *GORK*, *MRP5*), and stomatal movement (*NFYA5*, *MYB61*; Gray, 2005; Cominelli et al., 2010) were downregulated; (3) the generation and of NO and H_2O_2, key molecules mediating ABA- and dark-induced stomatal closure (Neill et al., 2008; Fujii and Zhu, 2009; Nakashima et al., 2014), was impaired. One can consider a pleiotropic nature of silencing *MPK4*, due to in Arabidopsis the *mpk4* mutant is highly pleiotropic and the absence of *MPK4* is monitored by the plant immune system and by the NB-LRR protein SUMM2 (Zhang et al., 2012). This gives rise to a number of phenotypes, such as small size and SA accumulation, which could be not directly regulated by MPK4. More targeted approaches (the lines with *MPK4* specifically silenced in GCs) would assess the role in GC function clearly to avoid effects possibly associated with pleiotropy. However, *mpk4* lines had

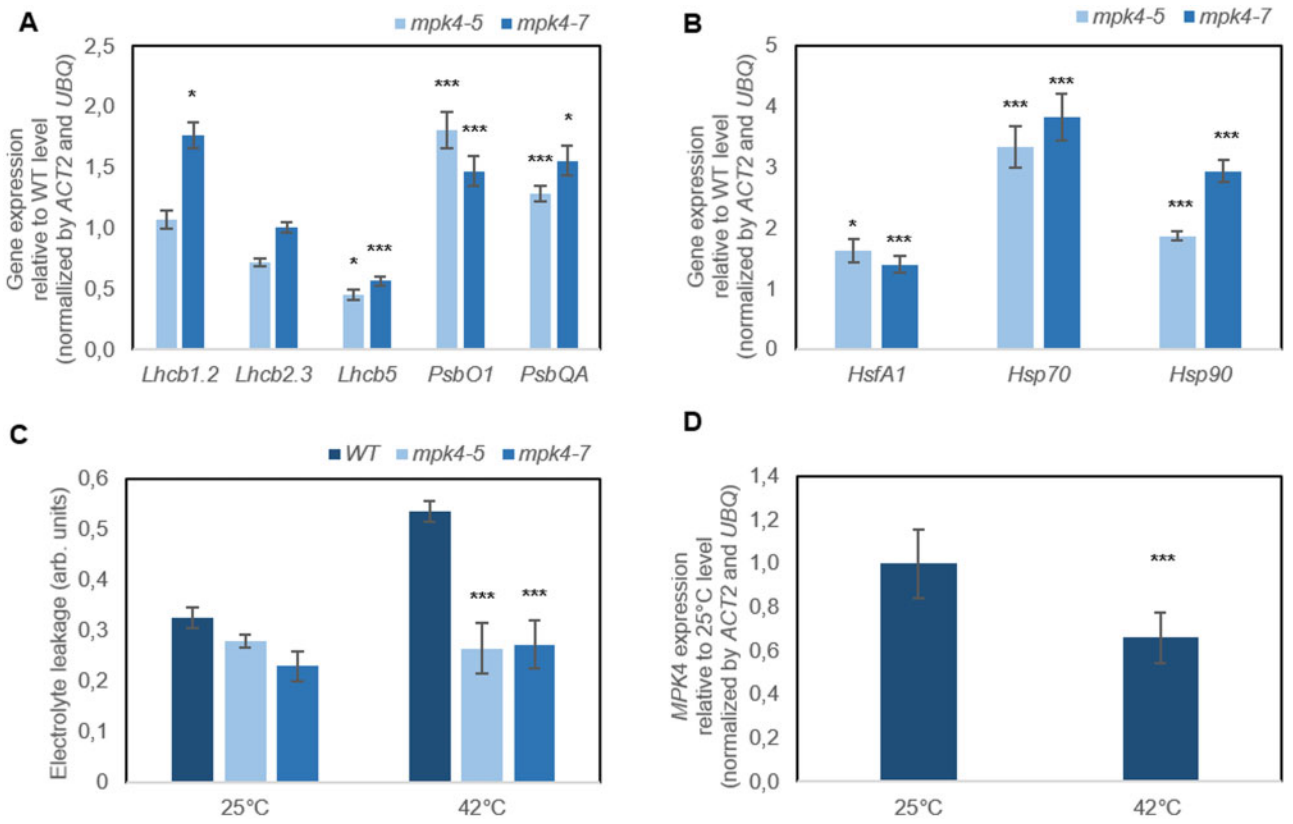

Figure 6 Photoprotection and cell death inhibition in transgenic *mpk*4-5 and *mpk*4-7 plants in comparison to WT plants. A, Relative expression of *Lhcb* and *PSB* in *mpk4* plants. B, Expression of HSF and HSP in *mpk4* plants. The expression levels in (A) and (B) are presented relative to that in WT control plants, referred to as 1.0. C, High-temperature response expressed as leaf electrolyte leakage. The values on figures (A–C) are the means ± SDs ($n = 6$). The asterisks indicate significant differences from the WT, as revealed by Tukey's HSD test; *$P < 0.05$, ***$P < 0.001$. D, High temperature induced a response in the expression of the *MPK4* gene in WT plants. The values are the means ± SDs ($n = 6$). The asterisks indicate significant differences from 25°C revealed by Tukey's HSD test; ***$P < 0.001$.

unambiguously specific phenotype, and even if MPK4 was in a network of relationships with other molecular factors, it can regulate the most important plant mechanisms at the level of physiology, metabolism, and cell signaling (Gawroński et al., 2014).

The direct and indirect effects of MPK4 in the stomata resulted in responses to a wide range abiotic stress conditions, including high and low temperatures, HCO_2 levels, light (high light, RL, RL/BL), drought, and phytohormonal (auxin, gibberellin, SA) regulation, as was found by in silico analysis of CREs and suggested by analysis of the *MPK4* expression level. In addition to the functioning of MPK4 as a positive regulator of ABA- and dark-dependent stomatal closure and its involvement in H_2O_2/NO signaling pathways, the permanently opened stomata were found in response to ABA, NO, H_2O_2, and dark treatment in *mpk4-7* transgenic plants. This suggests that the *MPK4* expression level is under environmental control, similar to the previously described activity of MPK4 (Teige et al., 2004; Marten et al., 2008; Wang et al., 2014) and other MAPKs, for example, MPK3 and MPK6 (Nakagami et al., 2005; Pitzschke and Hirt, 2006), in different species. Taken together, *MPK4*-dependent changes in hybrid aspen GCs are controlled on a surprisingly large number of levels, although it seems that one mechanism would be sufficient for maintenance of permanent stomatal opening in *mpk4* plants.

It can be concluded that MPK4 influences cell death/growth regulation and acclimation/defense pathways through long-term (stomatal density, leaf development, GC wall differentiation) and short-term (stomatal aperture) stomatal responses in natural field conditions. In *mpk4* plants, the final efficiency of primary PSII photochemistry and electron transport (φP_0, $\varphi E0$, F_v/F_0, ψ_0) was lowered, despite the trapped energy flux and electron transport per reaction center (RC; TR_0/RC, ET_0/RC) being higher. This resulted in H_2O_2 overproduction in leaf mesophyll and vein tissues (Witoń et al., 2016) and in turn in decreased plant biomass, particularly wood tissue in the stem, leaf size, and plant height (Witoń et al., 2016; Ślesak et al., 2013). At the same time, the light energy absorbed (ABS/RC) by *mpk4* plants was greater than that absorbed by WT plants, thus increasing energy dissipation and leaf temperature in the *mpk4* plants. The permanently open stomata did not prevent temperature deregulation. In the growing season, plants cultivated in the field tend naturally to absorb more light energy than they utilize for photosynthesis (Szechyńska-Hebda

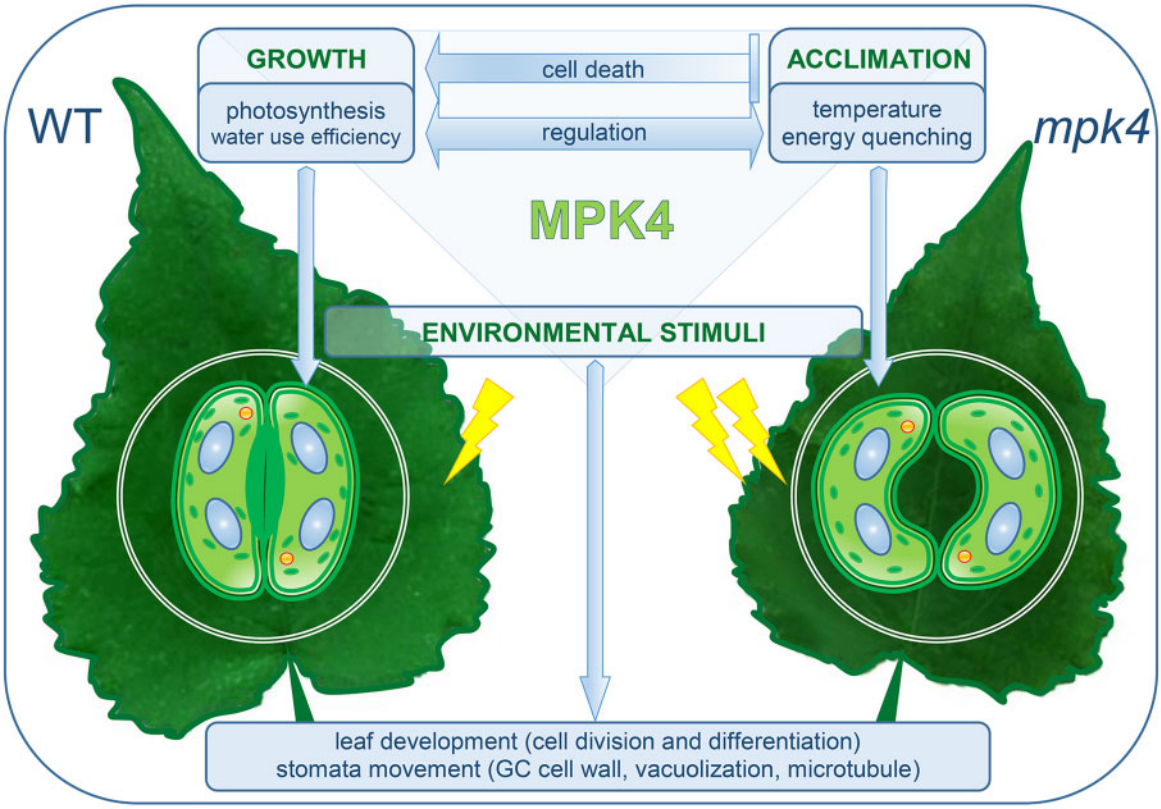

Figure 7 MPK4-dependent developmental and physiological mechanisms that balance growth and acclimatory responses. MPK4 deficiency in transgenic *mpk4* plants led to increased energy absorption, an increase in temperature, permanently open stomata, and an acclimation response, for example, energy dissipation as heat, and thus in an energy deficit in the CO_2 assimilation process and impaired accumulation of biomass; MPK4 is involved in processes that balance the distribution of photosynthetic energy between growth and acclimation/defense responses. WT, hybrid aspen T89 plants; *mpk4*—transgenic aspen plants. A list of acclimation and growth responses/mechanisms affected by MPK4 is presented in Supplemental Figure S9.

et al., 2015, 2016; Kulasek et al., 2016; Górecka et al., 2020). This energy absorbed in excess (excess excitation energy, EEE) has to be dissipated and quenched by NPQ mechanisms (Karpinski et al., 1999; Szechyńska-Hebda et al., 2010; Kulasek et al., 2016; Górecka et al., 2020). To reduce PSII photoinhibition in *mpk4* plants, acclimation responses were induced: increased chlorophyll and carotenoid levels, an effective antioxidant system (Witoń et al., 2016), a dissipation mechanism (DI_0/RC, φD_0), repair or de novo assembly of PSII (*Lhcb1*, *PsbO1*, and *PSBQA*), and HSFs and proteins (*HSFA1a*, *HSP70*, *HSP90*). These factors were responsible for the reduction in plant cell death during stress conditions (ion leakage; Gawroński et al., 2021). On the one hand, the EEE and higher foliar temperature of *mpk4* plants can be considered a part of both acclimation and defense mechanisms. EEE induces systemic acquired acclimation to abiotic stress (SAA), and simultaneously SAR to pathogens (Karpinski et al., 1999; Mühlenbock et al., 2008; Szechyńska-Hebda et al., 2010). The induction of SAA and SAR requires increased foliar content of free SA, elevated cellular ROS levels and antioxidant enzyme activities, adjusted photosynthesis (Karpinski et al., 1999; Mühlenbock et al., 2008; Szechyńska-Hebda et al., 2010; Szechyńska-Hebda et al., 2015, 2016), SA- and H_2O_2-dependent changes in the cell wall and consequently impaired plant growth (Szechyńska-Hebda et al., 2013, 2016; Ślesak et al., 2013), and additional molecular switches working in a light-dependent manner (e.g. Karpinski et al., 1999; Ślesak et al., 2013; Dąbrowska-Bronk et al., 2016). All these factors corresponded to silencing of the *MPK4* gene (Witoń et al., 2016; and results presented here). Similarly, the *A. thaliana mpk4* null mutant exhibited a highly elevated foliar SA level and, as a consequence, a dwarf phenotype and constitutive SAR to bacterial and oomycete pathogens (*Pseudomonas syringae* pv. tomato and *Phytophthora parasitica*, respectively; Petersen et al., 2000). Therefore, taking into consideration that in *mpk4* plants: (1) despite a lower total number of RCs, a higher energy absorption was noted as an effect of a higher total number of photons absorbed by Chl molecules in all RCs (increased ABS/RC) and an increased antenna size (Witoń et al., 2016; 1.3- to 2-fold higher chlorophyll content); (2) the temperature of leaves increased and permanently opened stomata together with higher energy dissipation prevented photoinhibition (acclimation response), however, this led to energy limiting for photochemistry (φP_0, $\varphi E0$, F_v/F_0, ψ_0 decline) followed by a reduction in the CO_2 assimilation process (decreased P.I.) and thus to impaired accumulation of biomass (impaired wood formation

in the stem, growth reduction); (3) the effective induction of different protecting mechanisms (DI_0/RC, φD_0 increase; Lhcb1, PsbO1, PSBQA repair; HSFA1a, HSP70, HSP90 induction; cell death reduction) and reduction in MPK4 levels in stress conditions were observed. Taken together, the points suggest that MPK4 is involved in processes that balance the distribution of photosynthetic energy between growth and acclimation/defense responses (Figure 7). Therefore, deregulation of MPK4 in transgenic *mpk4* plants leads to the redirection of light energy to mechanisms of heat dissipation thus temperature elevation and acclimatization, including increased tolerance to sudden temperature changes or excessive light intensity. In contrast, in WT plants with functional MPK4, energy is instead redirected to growth, and the acclimatization mechanisms are supported by other pathways, for example, induction of SA, ABA, cell death, SAA, and SAR.

Conclusions

We postulate that MPK4 in the hybrid aspen is an important regulatory hub that integrates responses to various external stimuli and leads to optimization of growth, acclimation, and defense responses through the multilevel regulation of stomatal movement and development and influencing of dissipation as a heat of absorbed energy by PSs.

Materials and methods

Plant material and growth conditions

Transgenic genotypes in the background of hybrid aspen (*P. tremula* × *tremuloides*) T89 (WT) were obtained in the Umeå Plant Science Centre (Umeå, Sweden) using the transformation procedure described by Nilsson et al. (1992). The construct for *MPK4* (XM_002320782.1), silencing was prepared based on RNA interference with the binary vector pH7GWIWG2(I) under the control of the 35S promoter and "Gateway" technology (Karimi et al., 2002). Eight *MPK4*-silenced lines were obtained from independent transformation events. Two of them, namely, *mpk4*-5 and *mpk4*-7, showed reduced expression of *MPK4* (by 25% and 90%, respectively; Witoń et al., 2016). Transgenic and WT trees were grown for 9 months in the greenhouse and were then transferred to the natural conditions in the "Wolica" experimental field (52° 8′30″N, 21°4′12″E) for 4 years (Supplemental Figure S1). Experiments were performed on 2- and 3-year-old hybrid aspen trees.

Light and transmission electron microscopy

Leaf samples were fixed and processed according to Gawroński et al. (2014) and Witoń et al. (2016). Semithin sections were analyzed under a light microscope (Olympus-Provis), and thin sections were analyzed under a transmission electron microscope (Morgagni 268D). Stem sections were prepared according to Szechyńska-Hebda et al. (2013, 2015). The tissues were analyzed under UV fluorescence (excitation filter 365 nm, dichroic mirror 395 nm, barrier filter 420 nm) and white light with a Nikon Eclipse E600 microscope equipped with a digital camera DXM 1200F.

Stomatal density

Epidermal strips from fully expanded young leaves were peeled from the abaxial and adaxial sides of the leaves. The epidermal strips were examined under a light microscope (Leica LMD 6000) equipped with a CCD camera and a workstation to determine the number of stomatal pores per square millimeter. Data are shown as the means ± standard deviations (SDS) of at least three independent experiments.

Immunolocalization

Fixation, embedding in butyl-methyl methacrylate resin, and sectioning were performed according to the method described by Sujkowska-Rybkowska and Borucki (2015). After resin removal with acetone, sections were incubated in blocking solution (3% BSA in 0.01 M phosphate-buffered saline [PBS], w/v) for 1 h at room temperature and then incubated in a solution containing primary antibody (anti-MPK4) diluted 1:100 with 1% BSA/0.01 M PBS (w/v) overnight at 4°C before washing in PBS and application of secondary (1:100) sheep anti-rabbit antibody conjugated to FITC (Sigma, St Louis, MO) in 0.01 M PBS for 1 h. The primary antibody was kindly provided by Professor Ichiro Mitsuhara (National Institute of Agrobiological Sciences, Ibaraki, Japan). Control sections were incubated without the primary antibody.

Two different primary antibodies, namely, JIM5 de-esterified HG and JIM7 high methyl-esterified HG (Plant Probes), were used for the immunodetection of pectin antigens (Knox, 1997; Willats et al., 2001). JIM12 was used for the immunodetection of the extensin epitope (Smallwood et al., 1994). Nonspecific binding of JIM5, JIM7, and JIM12 antibodies was tested by the omission of the primary antibody, and no labeling was found. JIM5, JIM7, and JIM12 antibodies were diluted 1:3 with 1% BSA/0.01 M PBS (w/v) overnight at 4°C before washing in PBS and application of secondary (1:200) goat anti-rat antibody conjugated to FITC (Sigma) in 0.01 M PBS for 1 h. For immunodetection of tubulin antigens in GCs, anti-alpha tubulin primary antibodies diluted 1:200 with 1% BSA/0.01 M PBS (w/v) were incubated overnight at 4°C before washing in PBS and application of secondary (1:200) goat anti-mouse antibody conjugated to Alexa Fluor 488 (Sigma) in 0.01 M PBS for 1 h. The sections were covered with a drop of distilled water and examined with confocal laser scanning microscope (Leica TCS SP5II; Leica Microsystems, Wetzlar, Germany). Fluorescence was excited by 488 nm argon laser and laser power ranging from 21% to 24% intensity and detected at 495–519 nm with the gain of the detector set to 100. The pinhole was maintained at 1 Airy Unit. The experiments were repeated three times to confirm the repeatability of the results.

Stomatal bioassays

The stomatal closure experiments were performed with freshly detached leaves as described previously

(He et al., 2013). Briefly, the leaves were first allowed to float on MES-KCl buffer "opening solution" (10 mM MES, 0.1 mM $CaCl_2$, 50 mM KCl, pH 6.15) with their abaxial surfaces facing up under white light (150 μmol m^{-2} s^{-1}) for 2 h to induce stomatal opening. Then, the leaves were allowed to float for 2 h in the buffer alone (control) or with 10 μM ABA (Sigma-Aldrich, St Louis, MO), 10 mM H_2O_2 (Sigma-Aldrich), or 50 μM SNP (Sigma-Aldrich) under the same light conditions (see above) or, to test dark-induced stomatal closure, the leaves were allowed to float in the buffer in the dark for 2 h. After the treatments, the abaxial epidermis was stripped from the leaves, and the stomatal pore size was measured with a calibrated light microscope. The data are shown as the means ± SDS of at least three independent experiments, each with 60 stomata.

Cytochemical determination of NO and H_2O_2

NO and H_2O_2 measurements were performed by using 4-amino-5-methylamino-2′,7′-difluorofluorescein (DAF-FM) diacetate (Thermo Fisher Scientific, Waltham, MA) and 2,7-dichlorofluorescein diacetate (H2DCF-DA; Sigma-Aldrich), respectively. Epidermal strips were incubated for ca. 2 h in MES/KCl buffer. After this step, the strips were loaded with 10 μM DAF-2DA for 10 min, followed by a wash step (with MES/KCl buffer) for 20 min. The strips were subsequently incubated in buffer alone or treated with 10 μM ABA or 50 μM SNP for various durations, as indicated in the text, before imaging. Fluorescence intensity maps were measured using a Zeiss Axio Observer Z1 equipped with LSM700 module and PTM detector. Fluorescence was excited by 488 nm laser set at 3%. The pinhole diameter was 33 μm. The excitation was reflected by a dichroic beam splitters (MBS 405/488561/639, DBS1: 567 nm, FW1: ET 525). Fluorescence of the DAF-FM was filtered using a narrow-band pass filter (SP 555 Zeiss). The gain of the detector was set to 1,126. For H2DCF-DA fluorescence intensity fluorescence was excited with a 488 nm laser with a laser power of 3%. The pinhole diameter was 40 μm. The excitation was reflected by a dichroic beam splitters (MBS 405/488561/639, DBS1: 567 nm, FW1: ET 525). Fluorescence of the H_2DCF-DA was filtered using band pass filter (BP 507-561 YFP). The gain of the detector set to 530. Data acquired from the confocal microscope were analyzed by using Scion Image software (ZEN lite; Zeiss, Oberkochen, Germany). The data are presented either as a percentage of fluorescence intensities of control-treated GCs or as average intensities from several GCs analyzed in different experiments.

Bioinformatic analysis of the MPK4 promoter

The promoter sequence upstream of the coding sequence of *MPK4* (*XM_002302563.2*) was extracted from the Phytozome (www.phytozome.net) genome database (Supplemental Table S4). CREs in the 1,000-bp promoter region were identified using the PlantCARE (bioinformatics.psb.ugent.be/webtools/plantcare/html/) and PLACE (www.dna.affrc.go.jp/PLACE/) databases. The distribution of CREs in the promoter sequence of the *MPK4* from *P. trichocarpa*, the closest relative of *P. tremula* × *tremuloides*, was used because of the lack of a promoter sequence for *P. tremula* × *tremuloides* in the available databases. The genomic sequence 1 kb upstream from the translation start site of *MPK4* was used in the promoter prediction software.

RNA isolation and RT-qPCR analysis

Total RNA was extracted from leaves using Concert™ Plant RNA Reagent (Invitrogen, Carlsbad, CA) according to the manufacturer's instructions. Samples were subjected to DNase I treatment with a DNA-free kit (Ambion, Applied Biosystems, Waltham, MA) for 30 min. The total RNA concentration was determined using a UV–Vis spectrophotometer (Thermo Scientific, NanoDrop). Reverse transcription reactions for cDNA synthesis were performed on 2 μg of RNA using a High Capacity cDNA Reverse Transcription Kit (Applied Biosystems, Foster City, CA) according to the manufacturer's instructions. Real-Time quantitative Polimerase Chain Reaction (RT-qPCR) was performed using a 7500 Fast Real-Time RT-PCR System (Applied Biosystems) according to the manufacturer's instructions. Relative transcript levels were determined using 7500 Software (Applied Biosystems) by normalizing the threshold cycle number of each gene with that of the aspen actin 2 (ACT2) and ubiquitin (UBQ) reference genes. Relative gene expression was calculated using the delta cycle threshold (CT) method. The delta CT value is the difference in CT between the gene of interest and the endogenous control for a given sample. Differences between the delta CT of a particular gene for an experimental sample and the delta CT of the same gene for the calibration sample were used for the calculation of relative gene expression level. The primer sequences used in this work are shown in the Supplemental materials (Supplemental Table S5). Each RT-qPCR was performed for two biological samples run in three technical repeats. RT-qPCR efficiency was calculated with the LinRegPCR tool (Ramakers et al., 2003).

High- and low-temperature treatment

Healthy, well-hydrated WT plants from the greenhouse were transferred to a growth chamber (light intensity, photons of 150 μmol m^{-2} s^{-1}) at 42°C or 4°C. After 2 h of treatment, the third, fourth, and fifth leaves from the top were collected and stored at −80°C.

Light treatment

Healthy, well-hydrated WT plants were illuminated with high light (Light 1), that is photons of 2,000 μmol m^{-2} s^{-1} of white light per 1 h, photons of 100 μmol m^{-2} s^{-1} of RL (Light 2) per 2 h or RL supplemented with photons of 20 μmol m^{-2} s^{-1} of BL per 2 h (Light 3). LED Lamps SL 3500-W-D (Photon System Instruments, Brno, Czech Republic) were used for experiments with plant illumination (red, 620 nm; royal blue, 455 nm). For dark treatment, WT plants were transferred to a closed paperboard box for 2 h. All experiments were performed at 21°C. After light or dark treatment, the third, fourth, and fifth leaves from the top were collected and stored at −80°C.

HCO_2 treatment

For HCO_2 conditions, the healthy, well-hydrated WT plants were transferred to a growth chamber (light intensity, photons of 150 µmol m^{-2} s^{-1}) with 2,000 ppm CO_2 for 2 h. After HCO_2 treatment, the third, fourth, and fifth leaves from the top were collected and stored at −80°C. WT plants cultivated in white light (photons of 150 µmol m^{-2} s^{-1}) at 21°C and in ambient CO_2 were used as a control.

DAB staining

H_2O_2 accumulation was visualized with DAB staining in whole leaves and leaf fragments. Microphotographs of a leaf were obtained with a light and fluorescence microscope (Eclipse E800, UV-2A, and EX330-380; 100×).

Electrolyte leakage

Leaf discs were incubated in the water bath at 42°C for 60 min. Leaf discs were then analyzed for electrolyte leakage as described by Suzuki et al. (2013). Control plants were untreated and leaf discs came from 25°C.

Statistical analysis

Statistics for all the results are presented as the means ± SDs. The biological replicates consisted of samples from at least three different trees for each genotype (*mpk4*-5, *mpk4*-7, and WT). Additionally, the mean of two lines *mpk4*-5 and *mpk4*-7 was calculated for all parameters. The significant differences were revealed by Tukey's HSD test. Statistical analysis was performed in STATGRAPHICS Plus version 5.1, GraphPad Prism version 5.03, or R version 2.13 software.

Accession numbers

UBQ (POPTR_001G418500), *ACT2* (POPTR_0001s31700), *COP1* (POPTR_0014s15740), *CRY1* (POPTR_0002s09730), *CRY2* (POPTR_0005s17100), *PHYA* (*POPTR_0013s00220*), *FAMA* (*POPTR_0017s08160*), *MYB88* (*POPTR_0010s10310*), *MYB61* (*POPTR_0005s00340*), *NFYA5* (*POPTR_0006s14740*), *ALMT12* (*POPTR_0001s02700*), *MRP5* (*POPTR_0014s18670*), *OST1* (*POPTR_0004s15270*), *SLAC1* (*POPTR_0005s20240*), *SLAH3* (*Potri.015G026700*), *RBOH D* (*POPTR_0003s15810*), *GORK* (*POPTR_0017s02430*), *HSP70* (*POPTR_0010s21350*), *HSP90* (*POPTR_0017s01160*), *HSFA1* (*POPTR_0001s02140*), *LHCB1.2* (*POPTR_0005s26080*), *LHCB2.3* (*POPTR_0014s16300*), *LHCB5* (*POPTR_0019s09140*), *PSBO1* (*POPTR_0005s13860*), *PSBQA* (*POPTR_0004s03160*), and *MPK4* (*POPTR_0002s16400*; Supplemental Table S5).

Supplemental data

The following materials are available in the online version of this article.

Supplemental Figure S1. WT and *mpk4* phenotype.

Supplemental Figure S2. MPK4 localization in the cytoplasm of GCs.

Supplemental Figure S3. No antibody control for Figure 2.

Supplemental Figure S4. Anti-tubulin antibody for MT distribution in WT, and transgenic *mpk4*-7 GC wall.

Supplemental Figure S5. *MPK4* expression under environmental control.

Supplemental Figure S6. Unaffected ABA-induced H_2O_2 accumulation in transgenic *mpk4*-7 GCs, and impaired ABA- and SNP-induced NO production in *mpk4*-7 GCs, when compared to WT GCs.

Supplemental Figure S7. H_2O_2 content in main veins and interveinal part of the leaf.

Supplemental Figure S8. Growth of *mpk4* plants.

Supplemental Figure S9. List of acclimation and growth responses/mechanisms affected by MPK4.

Supplemental Table S1. Cell number, area, and the circularity index in WT, transgenic *mpk4*-5, and *mpk4*-7 plants.

Supplemental Table S2. In silico analysis of the CREs distribution in the *MPK4* promoter of *P. trichocarpa* under different environmental stimuli.

Supplemental Table S3. In silico analysis of the CREs distribution in the *MPK4* promoter of *P. trichocarpa* under different hormonal stimuli.

Supplemental Table S4. The promoter sequence upstream the coding sequence of *MPK4*.

Supplemental Table S5. List of primers used in RT-qPCR.

Acknowledgments

The authors acknowledge the methodological and technical support provided by Maria Lewandowska, Maciej Jerzy Bernacki, Paweł Burdiak, Piotr Gawroński, and Ireneusz Ślesak from SGGW, and Professor E. Mellerowicz for supervising aspen transformation at the Umeå Plant Science Centre.

Funding

The research was supported by the PBS1/A8/16/2013 and BIOSTRATEG2/298241/10/NCBR/2016 projects granted by the National Centre for Research and Development, OPUS 15 2018/29/B/NZ3/01198 granted by the National Science Centre (to Stanislaw Karpinski), and Maestro 6 project UMO-2014/14/A/NZ1/00218 granted by the National Science Centre.

Conflicts of interest statement. The authors declare no conflicts of interest.

References

Amsbury S, Hunt L, Elhaddad N, Baillie A, Lundgren M (2016) Stomatal function requires pectin de-methyl esterification of the guard cell wall. Curr Biol **26**: 2899–2906

Bright J, Desikan R, Hancock JT, Weir IS, Neill SJ (2006) ABA-induced NO generation and stomatal closure in *Arabidopsis* are dependent on H_2O_2 synthesis. Plant J **45**: 113–122

Brownlee C (2001) The long and the short of stomatal density signals. Trends Plant Sci **6**: 441–442

Cannon MC, Terneus K, Hall Q, Tan L, Wang Y, Wegenhart BL, Chen L, Lamport DT, Chen Y, Kieliszewski MJ (2008) Self-assembly of the plant cell wall requires an extensin scaffold. Proc Natl Acad Sci USA **105**: 2226–2231

Colcombet J, Berriri S, Hirt H (2013) Constitutively active MPK4 helps to clarify its role in plant immunity. Plant Signal Behav **8**: e22991

Cominelli E, Galbiati M, Tonelli C (2010) Transcription factors controlling stomatal movements and drought tolerance. Transcription **1**: 41–45

Dąbrowska-Bronk J, Komar D, Rusaczonek A, Kozłowska-Makulska A, Szechyńska-Hebda M, Karpiński S (2016) β-carbonic anhydrases and carbonic ions uptake positively influence *Arabidopsis* photosynthesis, oxidative stress tolerance and growth in light dependent manner. J Plant Physiol **203**: 44–54

Dillen SY, Marron N, Koch B, Ceulemans R (2008) Genetic variation of stomatal traits and carbon isotope discrimination in two hybrid poplar families (*Populus deltoides* 'S9-2' × *P. nigra* 'Ghoy' and *P. deltoides* 'S9-2' × *P. trichocarpa* 'V24'). Ann Bot **102**: 399–407

Dyda M, Wąsek I, Tyrka M, Wędzony M, Szechyńska-Hebda M (2019) Local and systemic regulation of PSII efficiency in triticale infected by the hemibiotrophic pathogen *Microdochium nivale*. Physiol Plant **165**: 711–727

Foyer CH and Noctor G (2020) Redox homeostasis and signalling in a higher-CO_2 world. Ann Rev Plant Biol **71**: 157–182

Fujii H, Zhu JK (2009) *Arabidopsis* mutant deficient in 3 abscisic acid-activated protein kinases reveals critical roles in growth, reproduction, and stress. Proc Natl Acad Sci USA **106**: 8380–8385

Gałgańska H, Gałgański L (2020) Mitogen-activated protein kinases are carbon dioxide receptors in plants. BioRxiv doi: 10.1101/2020.05.09.086116

Gawroński P, Burdiak P, Scharff LB, Mielecki J, Górecka M, Zaborowska M, Leister D, Waszczak C, Karpiński S (2021) CIA2 and CIA2-LIKE are required for optimal photosynthesis and stress responses in *Arabidopsis thaliana*. Plant J **105**: 619–638

Gawroński P, Witoń D, Vashutina K, Bederska M, Betliński B, Rusaczonek A, Karpiński S (2014) Mitogen-activated protein kinase 4 is a salicylic acid-independent regulator of growth but not of photosynthesis in *Arabidopsis*. Mol Plant **7**: 1151–1166

Gomi K, Ogawa D, Katou S, Kamada H, Nakajima N, Saji H, Soyano T, Sasabe M, Machida Y, Mitsuhara I, et al. (2005) A mitogen-activated protein kinase NtMPK4 activated by SIPKK is required for jasmonic acid signaling and involved in ozone tolerance via stomatal movement in tobacco. Plant Cell Physiol **46**: 1902–1914

Górecka M, Lewandowska M, Dąbrowska-Bronk J, Białasek M, Barczak-Brzyżek A, Kulasek M, Mielecki J, Kozłowska-Makulska A, Gawroński P, Karpiński S (2020) Photosystem II 22kDa protein level—a prerequisite for excess light-inducible memory, cross-tolerance to UV-C and regulation of electrical signalling. Plant Cell Environ **43**: 649–661

Gray J (2005) Guard cells: transcription factors regulate stomatal movements. Curr Biol **15**: R593–595

He JM, Ma XG, Zhang Y, Sun TF, Xu FF, Chen YP, Liu X, Yue M (2013) Role and interrelationship of Gα protein, hydrogen peroxide, and nitric oxide in ultraviolet B-induced stomatal closure in *Arabidopsis* leaves. Plant Physiol **161**: 1570–1583

Hettenhausen C, Baldwin IT, Wu J (2012) Silencing MPK4 in *Nicotiana attenuata* enhances photosynthesis and seed production but compromises abscisic acid-induced stomatal closure and guard cell-mediated resistance to *Pseudomonas syringae* pv tomato DC3000. Plant Physiol **158**: 759–776

Karimi M, Inzé D, Depicker A (2002) GATEWAY vectors for *Agrobacterium*-mediated plant transformation. Trends Plant Sci **7**: 193–195

Karpinski S, Reynolds H, Karpinska B, Wingsle G, Creissen G, Mullineaux P (1999) Systemic signaling and acclimation in response to excess excitation energy in *Arabidopsis*. Science **284**: 654–657

Kim TH, Böhmer M, Hu H, Nishimura N, Schroeder JI (2010) Guard cell signal transduction network: advances in understanding abscisic acid, CO_2, and Ca2+ signaling. Annu Rev Plant Biol **61:** 561–591

Knox JP (1997) The use of antibodies to study the architecture and developmental regulation of plant cell walls. Int Rev Cytol **171**: 79–120

Kulasek M, Jerzy Bernacki M, Ciszak K, Witoń D, Karpiński S (2016) Contribution of PsbS function and stomatal conductance to foliar temperature in higher plants. Plant Cell Physiol **57**: 1495–1509

Kwak JM, Mori IC, Pei ZM, Leonhardt N, Torres MA, Dangl JL, Bloom RE, Bodde S, Jones JD, Schroeder JI (2003) NADPH oxidase AtrbohD and AtrbohF genes function in ROS-dependent ABA signaling in *Arabidopsis*. EMBO J **22**: 2623–2633

Lionetti V, Cervone F, Bellincampi D (2012) Methyl esterification of pectin plays a role during plant-pathogen interactions and affects plant resistance to diseases. J Plant Physiol **169**: 1623–1630

Liu Y, Zhang C, Chen J, Guo L, Li X, Li W, Yu Z, Deng J, Zhang P, Zhang K, Zhang L (2013) *Arabidopsis* heat shock factor HsfA1a directly senses heat stress, pH changes, and hydrogen peroxide via the engagement of redox state. Plant Physiol Biochem **64**: 92–115

Marten H, Hyun T, Gomi K, Seo S, Hedrich R, Roelfsema MRG (2008) Silencing of *NtMPK4* impairs CO_2-induced stomatal closure, activation of anion channels and cytosolic Ca^{2+} signals in *Nicotiana tabacum* guard cells. Plant J **55**: 698–708

Mühlenbock P, Szechyńska-Hebda M, Plaszczyca M, Baudo M, Mullineaux PM, Parker JE, Karpińska B, Karpiński S (2008) Chloroplast signaling and LESION SIMULATING DISEASE1 regulate crosstalk between light acclimation and immunity in *Arabidopsis*. Plant Cell **20**: 2339–2356

Nakagami H, Pitzschke A, Hirt H (2005) Emerging MAP kinase pathways in plant stress. Trends Plant Sci **10**: 339–346

Nakashima K, Yamaguchi-Shinozaki K, Shinozaki K (2014) The transcriptional regulatory network in the drought response and its crosstalk in abiotic stress responses including drought, cold, and heat. Front Plant Sci **5**: 170

Neill S, Barros R, Bright J, Desikan R, Hancock J, Harrison J, Morris P, Ribeiro D, Wilson I (2008) Nitric oxide, stomatal closure, and abiotic stress. J Exp Bot **59**: 165–176

Nilsson O, Aldén T, Sitbon F, Little CHA, Chalupa V, Sandberg G, Olsson O (1992) Spatial pattern of cauliflower mosaic virus 35S promoter-luciferase expression in transgenic hybrid aspen trees monitored by enzymatic assay and non-destructive imaging. Transgenic Res **1**: 209–220

Petersen M, Brodersen P, Naested H, Andreasson E, Lindhart U, Johansen B, Nielsen HB, Lacy M, Austin MJ, Parker JE, et al. (2000) *Arabidopsis* map kinase 4 negatively regulates systemic acquired resistance. Cell **103**: 1111–1120

Pietrzykowska M, Suorsa M, Semchonok DA, Tikkanen M, Boekema EJ, Aro EM, Jansson S (2014). The light harvesting chlorophyll a/b binding proteins Lhcb1 and Lhcb2 play complementary roles during state transitions in *Arabidopsis*. Plant Cell **26**: 3646–3660

Pitzschke A, Djamei A, Bitton F, Hirt H (2009) A major role of the MEKK1–MKK1/2–MPK4 pathway in ROS signaling. Mol Plant **2**: 120–137

Pitzschke A, Hirt H (2006) Mitogen-activated protein kinases and reactive oxygen species signaling in plants. Plant Physiol **141**: 351–356

Ramakers C, Ruijter JM, Deprez RHL, Moorman AFM (2003) Assumption-free analysis of quantitative real-time polymerase chain reaction (PCR) data. Neurosci Lett **339**: 62–66

Rodriguez MCS, Petersen M, Mundy J (2010) Mitogen-activated protein kinase signaling in plants. Ann Rev Plant Biol **61**: 621–649

Shimazaki K, Doi M, Assmann SM, Kinoshita T (2007) Light regulation of stomatal movement. Annu Rev Plant Biol **58**: 219–247

Suzuki N, Miller G, Salazar C, Mondal HA, Shulaev E, Cortes DF, Shuman JL, Luo X, Shah J, Schlauch K, et al. (2013) Temporal-spatial interaction between reactive oxygen species and abscisic acid regulates rapid systemic acclimation in plants. Plant Cell **25**: 3553–3569

Ślesak I, Szechyńska-Hebda M, Fedak H, Sidoruk N, Dąbrowska-Bronk J, Witoń D, Rusaczonek A, Antczak A, Drożdżek M, Karpińska B, et al. (2013) PHYTOALEXIN DEFICIENT 4 affects

reactive oxygen species metabolism, cell wall and wood properties in hybrid aspen (*Populus tremula* L. × *tremuloides*). Plant Cell Environ **38**: 1275–1284

Smallwood M, Beven A, Donovan N, Neill SJ, Peart J, Roberts K, Knox JP (1994) Localization of cell wall proteins in relation to the developmental anatomy of the carrot root apex. Plant J **5**: 237–246

Sujkowska-Rybkowska M, Borucki W (2015) Pectins esterification in the apoplast of aluminum-treated pea root nodules. J Plant Physiol **184**: 1–7

Swamy PS, Hu H, Pattathil S, Maloney VJ, Xiao H, Xue LJ, Chung JD, Johnson VE, Zhu Y, Peter GF, et al. 2015. Tubulin perturbation leads to unexpected cell wall modifications and affects stomatal behaviour in *Populus*. J Exp Bot **66**: 6507–6518

Swindell WR, Huebner M, Weber AP (2007) Transcriptional profiling of *Arabidopsis* heat shock proteins and transcription factors reveals extensive overlap between heat and non-heat stress response. BMC Genomics **8**: 125

Szechyńska-Hebda M, Hebda M, Mierzwiński D, Kuczyńska P, Mirek M, Wedzony M, van Lammeren A, Karpiński S (2013) Effect of cold-induced changes in physical and chemical leaf properties on the resistance of winter triticale (×*Triticosecale*) to the fungal pathogen *Microdochium nivale*. Plant Pathol **62**: 867–878

Szechyńska-Hebda M, Czarnocka W, Hebda M, Karpiński S (2016) PAD4, LSD1 and EDS1 regulate drought tolerance, plant biomass production, and cell wall properties. Plant Cell Rep **35**: 527–539

Szechyńska-Hebda M, Wasek I, Gołebiowska G, Dubas E, Zur I, Wedzony M (2015) Photosynthesis-dependent physiological and genetic crosstalk between cold acclimation and cold-induced resistance to fungal pathogens in triticale (*Triticosecale* Wittm). J Plant Physiol **177**: 30–43

Szechyńska-Hebda M, Wedzony M, Dubas E, Kieft H, van Lammeren A (2006) Visualisation of microtubules and actin filaments in fixed BT-2 suspension cells using an optimised whole mount immunolabelling protocol. Plant Cell Rep **25**: 758–766

Szechyńska-Hebda M, Kruk J, Górecka M, Karpinska B, Karpinski S (2010) Evidence for light wavelength-specific photoelectrophysiological signaling and memory of excess light episodes in *Arabidopsis*. Plant Cell **22**: 2201–2218

Teige M, Scheikl E, Eulgem T, Dóczi R, Ichimura K, Shinozaki K, Dangl JL, Hirt H (2004) The MKK2 pathway mediates cold and salt stress signaling in *Arabidopsis*. Mol Cell **15**: 141–152

Töldsepp K, Zhang J, Takahashi Y, Sindarovska Y, Horak H, Ceciliato PHO, Koolmeister K, Wang Y-S, Vaahtera L, Jakobson L, et al. (2018) Mitogen-activated protein kinases MPK4 and MPK12 are keycomponents mediating CO_2-induced stomatal movements. Plant J **96**: 1018–1035

Wang F, Shang Y, Fan B, Yu JQ, Chen Z (2014) *Arabidopsis* LIP5, a positive regulator of multivesicular body biogenesis, is a critical target of pathogen-responsive MAPK cascade in plant basal defense. PLoS Pathog **10**: e1004243

Willats W, Orfila C, Limberg G, Buchholt HC, van Alebeek GJ, Voragen AG, Marcus SE, Christensen TM, Mikkelsen JD, Murray BS, et al. (2001) Modulation of the degree and pattern of methyl-esterification of pectic homogalacturonan in plant cell walls. J Biol Chem **276**: 19404–19413

Witoń D, Gawroński P, Czarnocka W, Ślesak I, Rusaczonek A, Sujkowska-Rybkowska, M, Bernacki MJ, Dąbrowska-Bronk J, Tomsia N, Szechyńska-Hebda M, et al. (2016) Mitogen activated protein kinase 4 (MPK4) influences growth in *Populus tremula* L.× *tremuloides*. Environ Exp Bot **130**: 189–205

Wituszyńska W, Gałązka K, Rusaczonek A, Vanderauwera S, Van Breusegem F, Karpiński S (2013) Multivariable environmental conditions promote photosynthetic adaptation potential in *Arabidopsis thaliana*. J Plant Physiol **170**: 548–559

Zeng Q, Chen JG, Ellis BE (2011) AtMPK4 is required for male-specific meiotic cytokinesis in *Arabidopsis*. Plant J **67**: 895–906

Zhang Z, Wu Y, Gao M, Zhang J, Kong Q, Liu Y, Ba H, Zhou J, Zhang Y (2012) Disruption of PAMP-induced MAP kinase cascade by a *Pseudomonas syringae* effector activates plant immunity mediated by the NB-LRR protein SUMM2. Cell Host & Microbe **11**: 253–263

Zoulias N, Harrison EL, Casson SA, Gray JE (2018) Molecular control of stomatal development. Biochem J **475**: 441–454